Studies on Novel Bone Resorption Inhibitors. II.[1] Synthesis and Pharmacological Activities of Fused Aza-heteroarylbisphosphonate Derivatives[2]

Makoto TAKEUCHI,*[,a] Shuichi SAKAMOTO,[a] Kousei KAWAMUKI,[b] Hiroyuki KURIHARA,[a] Hideaki NAKAHARA,[a] and Yasuo ISOMURA[a]

Institute for Drug Discovery Research, Yamanouchi Pharmaceutical Co., Ltd.,[a] 21 Miyukigaoka, Tsukuba, Ibaraki 305–8585, Japan and Clinical Development Division, Yamanouchi Pharmaceutical Co., Ltd., [b] 3–17–1 Hasune, Itabashi-ku, Tokyo 174–8612, Japan. Received May 21, 1998; accepted August 11, 1998

Two new series of fused aza-heteroarylbisphosphonates (5, 8), which are structurally quite different from incadronate (YM175), and related compounds were synthesized and evaluated for antiresorptive activity using a parathyroid hormone(PTH)-induced hypercalcemia model in rats (PIH model). Among these compounds, several exhibited more potent antiresorptive activity than pamidronate. In particular, [1-hydroxy-2-(imidazo[1,2-*a*]pyridin-3-yl)ethylidene]bisphosphonic acid (5b, minodronate) was 100-fold more potent than pamidronate in not only the PIH model, but also in an immobilization bone atrophy model in rats (DA model), and was selected for clinical development. The structure–activity relationships in these new series of bisphosphonates are discussed.

Key words bisphosphonate; incadronate; minodronate; pamidronate; bone resorption inhibitor; hypercalcemia

The geminal bisphosphonates, which are carbon analogs of pyrophosphate, exhibit antiresorptive activity *in vitro* and *in vivo*.[3,4] Bisphosphonates such as pamidronate (**1**) and alendronate (**2**) (Fig. 1), are therefore used for the treatment of disorders of bone mineral metabolism characterized by increased bone resorption, including Paget's disease, tumoral hypercalcemia, bone metastases and osteoporosis.[5] In a previous paper,[1] we reported that a series of (cycloalkylamino)methylenebisphosphonate derivatives, such as incadronate (YM175) (**3**),[6,7] showed potent antiresorptive activity, and suggested that the bulkiness and lipophilicity of the substituent on the nitrogen atom and the conformation of the compound were also important determinants of the antiresorptive activity. In the meantime, it has been reported that bisphosphonates which have imidazole rings (*e.g.* **4**, **7**), showed potent antiresorptive activity.[8,9] In order to further investigate the influence of not only the bulkiness and lipophilicity of the imidazole ring, but also the conformation of these compounds on antiresorptive activity, we envisaged the structural modifications of compounds **4** and **7** depicted in Fig. 2. Namely, with respect to compound **4**, attachment of a benzene or cyclohexane ring to the imidazole ring was carried out. On the other hand, with respect to compound **7**, the attachment of a imidazole or pyridine ring to the imidazole ring was carried out. These newly prepared bisphosphonates (**5**, **6**, **8**, **9**) were evaluated for their antiresorptive activities using the parathyroid hormone(PTH)-induced hypercalcemia model (PIH model). Among these compounds, [1-hydroxy-2-(imidazo[1,2-*a*]pyridin-3-yl)ethylidene]bisphosphonic acid (**5b**) showed the most potent inhibitory activity, and its activity was 100-fold more potent than that of pamidronate.

We describe here the synthesis and antiresorptive activities of two new series of fused aza-heteroarylbisphosphonates and related compounds.

Synthesis As shown in Chart 1, the 1-hydroxybisphosphonate derivatives (**5a—d**) listed in Table 1 were prepared from the corresponding carboxylic acids (**10a—d**) according to the method described in the literature.[10] Namely, treatment of the carboxylic acids (**10a—d**)[11—13] with phosphorous acid and phosphorus trichloride followed by hydrolysis under acidic conditions gave the desired 1-hydroxybisphosphonate derivatives (**5a—d**). The propanoic acid derivative

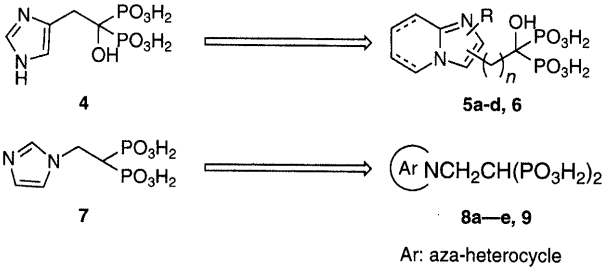

Fig. 2

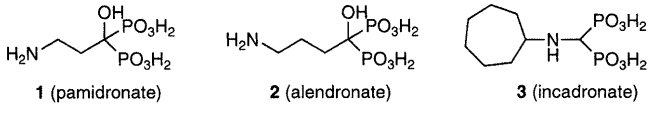

Fig. 1. Structures of Pamidronate, Alendronate and Incadronate

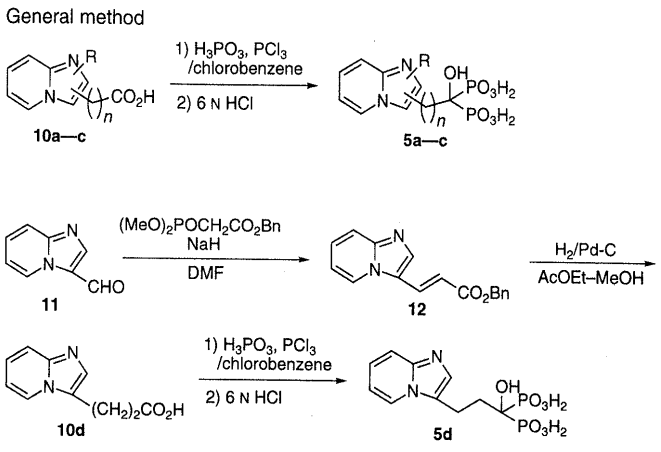

Chart 1

* To whom correspondence should be addressed.

Table 1. Physical Data for Bisphosphonates (**5**)

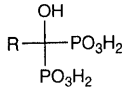

Compd.	R	Yield (%)	mp (°C) (Recryst. solv.)[a]	Formula	Analysis (%) Calcd (Found) C	H	N	P
5a	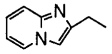	54.1	248—250 (L)	$C_9H_{12}N_2O_7P_2$	33.56 (33.33	3.75 3.69	8.70 8.67	19.23 19.13)
5b	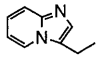	34.0	222—224 (dec.) (H–M)	$C_9H_{12}N_2O_7P_2 \cdot 0.5H_2O$	32.64 (32.45	3.96 3.91	8.46 8.65	18.71 19.05)
5c	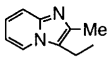	24.9	236—238 (H–M)	$C_{10}H_{14}N_2O_7P_2 \cdot 1.5H_2O$	33.07 (33.02	4.72 4.49	7.71 7.69	17.06 17.26)
5d	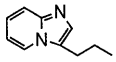	50.6	257—259 (L)	$C_{10}H_{14}N_2O_7P_2$	35.73 (35.70	4.20 4.27	8.33 8.25	18.43 18.33)

a) H: H_2O, L: 1 N HCl, M: methanol.

Table 2. Physical Data for Bisphosphonates (**8**)

$R\text{-}CH_2CH(PO_3H_2)_2$

Compd.	R	Method[a]	Yield (%)	mp (°C) (Recryst. solv.)[b]	Formula	Analysis (%) Calcd (Found) C	H	N	P
8a		A	60.3	257—258 (H–M)	$C_6H_{12}N_2O_6P_2$	26.68 (26.31	4.48 4.32	10.37 10.19	22.93 22.82)
8b		A	37.0	Amorphous	$C_6H_{12}N_2O_6P_2 \cdot H_2O$	25.01 (25.32	4.90 4.69	9.72 9.71	21.50 21.44)
8c		A	64.2	320—324 (dec.) (L)	$C_7H_{11}N_3O_6P_2 \cdot 0.2H_2O$	28.14 (27.95	3.85 3.60	14.07 13.97	20.74 20.52)
8d		A	86.0	252—254 (H–M)	$C_7H_{13}N_3O_6P_2$	28.30 (28.10	4.41 4.28	14.40 14.06	20.85 20.81)
8e		B	30.6	267—271 (H–M)	$C_8H_{11}N_3O_6P_2 \cdot 2H_2O$	28.00 (28.14	4.40 3.99	12.24 11.93	18.05 18.25)

a) A: c. HCl, B: TMSI. *b*) H: H_2O, L: 1 N HCl, M: methanol.

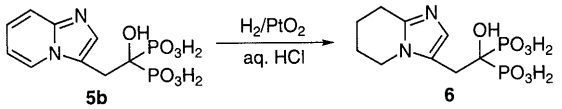

Chart 2

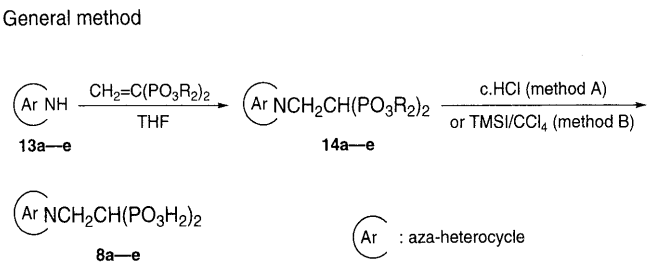

Chart 3

(**10d**), the starting material for compound **5d**, was prepared from imidazo[1,2-*a*]pyridine-3-carbaldehyde (**11**).[14] Treatment of **11** with benzyl dimethylphosphonoacetate in the presence of NaH produced the benzyl ester derivative (**12**). Subsequent hydrogenation of **12** gave the desired product **10d**. As shown in Chart 2, compound **5b** was hydrogenated in the presence of platinum oxide to afford the tetrahydroimidazo[1,2-*a*]pyridine derivative (**6**). The ethylidenebisphosphonate derivatives (**8a—e**) listed in Table 2 were prepared as shown in Chart 3. Treatment of the corresponding azoles (**13a—e**)[15—17] with tetraalkylethenylidenebisphosphonate[18] followed by hydrolysis of the tetraester (**14a—e**) with concentrated hydrochloric acid (method A) or iodotrimethylsilane (method B) gave the desired ethylidenebisphosphonate derivatives (**8a—e**). The synthetic method for the imidazo[4,5-*b*]pyridin-2-yl derivative (**9**) is shown in Chart 4. Treatment of tetraisopropyl methylenebisphosphonate (**15**) with benzyl 2-bromoacetate in the presence of NaH followed by hydrogenation of the benzyl ester (**16**) in the presence of palladium carbon under atmospheric hydrogen pressure afforded the debenzyl derivative (**17**). Compound **17** was treated with 2,3-diaminopyridine under acidic conditions to afford the desired bisphosphonate **9**.

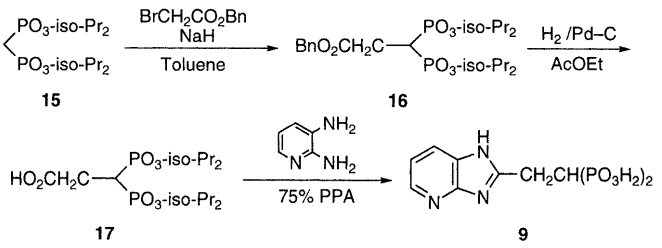

Chart 4

Results and Discussion

The antiresorptive activities of the bisphosphonates thus obtained were evaluated on the basis of their ability to reduce serum Ca^{2+} concentration in the PIH model in rats, as described in the Experimental section. The pharmacological results are listed in Tables 3 and 4. At first, we focused our efforts on investigating the conversion of the imidazole ring of compound **4** to the imidazo[1,2-*a*]pyridine ring and optimization of the attachment position of the benzene ring to the imidazole ring(Table 3). The imidazo[1,2-*a*]pyridin-2-yl derivative (**5a**) showed remarkably decreased potency, whereas the 3-yl derivative (**5b**), which has a similar clogP value,[19] showed the same potency as compound **4**. These results suggest that the attachment of a hydrophobic group such as a benzene ring, while increasing the lipophilicity, is well tolerated and maintains the antiresorptive activity, and that the activity is greatly affected by the attachment position of the benzene ring to the imidazole ring. In order to investigate the cause of the difference in potency between compounds **5a** and **5b**, we carried out X-ray crystallographic analysis of **5a** and **5b** monohydrate. The ORTEP II drawings of **5a** and **5b** monohydrate, and also the superimposition of **5a** and **5b** monohydrate are shown in Figs. 3, 4 and 5, respectively.[20] Based on the results of the X-ray crystallographic analysis, two important differences between compounds **5a** and **5b** were observed. One was the distance between the two phosphonate groups, which are crucial for antiresorptive activity, and the imidazo[1,2-*a*]pyridine ring, and the other was the interplanar angle between the least squares plane of the bisphosphonate group, composed of atoms P13–C11–P17, and that of the imidazo[1,2-*a*]pyridine ring. The distances between the center of the benzene ring of compound **5a** and the two phosphorus atoms (P13, P17) were 7.27 and 5.43 Å, respectively. On the other hand, those of compound **5b** were 6.45 and 4.62 Å, respectively.[21] The distances between the two phosphonate groups and the imidazo[1,2-*a*]pyridine ring of compound **5a** were longer in comparison with compound **5b**. Furthermore, the interplanar angles between the least squares plane of the bisphosphonate group and that of the imidazo[1,2-*a*]pyridine ring were 60.05 (12)° for compound **5a** and 42.93 (15)° for compound **5b**, respectively.[22] The least squares plane of the imidazo[1,2-*a*]pyridine ring of compound **5b** was more parallel to the plane of the bisphosphonate group than that of compound **5a**. Based on these results, we speculated that the hydrophobic moiety must have a preferable position, in terms of both adequate distance from the bisphosphonate group and interplanar angle to the plane of the bisphosphonate group, in order to provide potent antiresorptive activity. Namely, the conformation of the compound is an important determinant of the antiresorptive activity. Chain extension by one carbon (**5d**) dramatically decreased the activity in comparison to **5b**. This result supported our speculation. Surprisingly, introduction of a methyl group at the C-2 position of the imidazo[1,2-*a*]pyridine ring (**5c**) resulted in a drastic decrease in the activity. We can speculate two reasons for the low activity of **5c** compared with **5b**.The first is due to steric repulsion of the methyl group with a target molecule. The second is the high energy cost involved in forming the active conformation when the methyl group is introduced. In order to examine the latter hypothesis, a systematic search was carried out for **5b** and **5c**, to see if there were any differences between their conforma-

Table 3. Effects of 1-Hydroxybisphosphonate Derivatives in the PIH Model

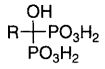

Compd.	R	clogP of R[a]	MED[b]
4		0.230	0.003
5a	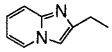	1.468	>0.1
5b	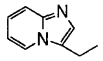	1.468	0.003
5c	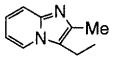	1.687	>0.3
5d	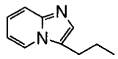	1.997	>0.3
6	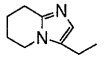	1.099	≦0.01
pamidronate (**1**)			0.3

a) The methylene and ethylene groups between aromatic rings and bisphosphonate groups were calculated as methyl and ethyl groups, respectively. *b*) mg/kg, s.c.

Table 4. Effects of Ethylidenebisphosphonate Derivatives in the PIH Model

R-$CH_2CH(PO_3H_2)_2$

Compd.	R	clogP of R-Me	MED[a]
7		−0.013	0.01
8a		0.256	0.1
8b		0.256	0.003
8c		0.425	≦0.03
8d		0.792	0.3
8e		0.473	>0.3
9		0.904	>0.1
pamidronate (**1**)			0.3

a) mg/kg, s.c.

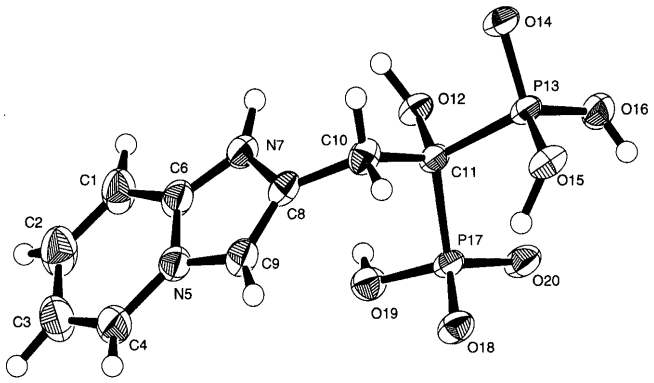

Fig. 3. Molecular Structure of Compound **5a**
Ellipsoids are drawn at the 50% probability level.

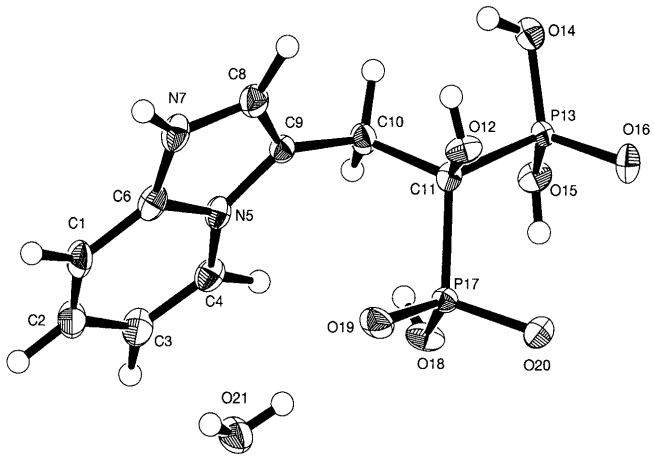

Fig. 4. Molecular Structure of Compound **5b** Monohydrate
Ellipsoids are drawn at the 50% probability level.

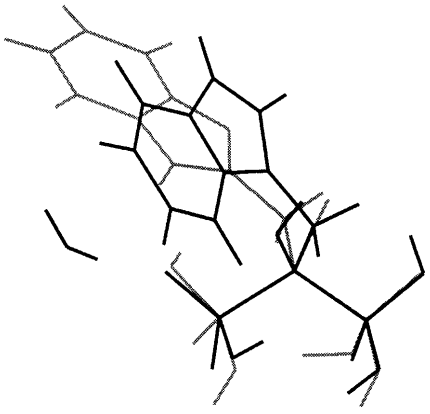

Fig. 5. Superimposition of Compound **5a** (Gray) and **5b** Monohydrate (Black)

tional energies. Since we have assumed that the crystal structure form is the active conformation, the crystal structure of **5b** was used for the calculations without energy minimization. Two rotatable bonds connecting the methyl and hydroxy groups were changed step by step, and more than one million conformers were generated for energy evaluation.

The results of the energy calculations for both compounds were quite similar, in spite of the allowed region for torsion angles being somewhat restricted for compound **5c**. The crystal structure of **5b** was a rather low-energy-conformer and its conformational energy did not change much even when introducing a methyl group to the aromatic ring. This means that compound **5c** is able to form an active conformation without much energy cost if the crystal structure is the active conformer. Therefore, the reason for the decrease in activity upon introduction of a methyl group is probably due to steric repulsion with a target molecule.

The conversion of the benzene ring (**5b**) into a cyclohexane ring (**6**) resulted in almost the same level of activity as that of compound **5b**. Concerning the hydrophobic group attached to the imidazole ring, this result suggests that the aromatic ring is not always indispensable for providing potent antiresorptive activity. Potency was extremely sensitive to minor changes in the chemical structure of the imidazo[1,2-*a*]pyridine moiety. The structure–activity relationships of this series described above, demonstrated that increase in lipophilicity by attachment of a hydrophobic group, such as a benzene or cyclohexane ring, to the imidazole ring was well tolerated and maintained the antiresorptive activity. However, the distance between the hydrophobic group and bisphosphonate group or the interplanar angles between the least squares plane of the bisphosphonate group and that of the imidazo[1,2-*a*]pyridine ring seemed to be very important determinants of the antiresorptive activity.

Next, we focused our efforts on investigating the introduction of a methyl group to the imidazole ring of compound **7** and conversion of the imidazole ring to various fused azaheteroaryl rings. These results are shown in Table 4. With regards to the introduction of methyl groups (**8a**, **8b**) to the imidazole ring of compound **7**, a large difference in potency was observed. The 4-methyl derivative (**8b**) was 30-fold more potent than the 2-methyl derivative (**8a**). This result suggests that increase of the lipophilicity is one means for increasing the antiresorptive activity, and that the activity is significantly influenced by the position of the substituent. We presume that the reason for the decrease in the potency of compound **8a** is similar to the case of compound **5c**, as already described. The imidazo[1,2-*a*]imidazole derivative (**8c**), which has greater lipophilicity than compound **7**, showed almost the same activity as **7**. The 2,3-dihydroimidazo[1,2-*a*]imidazole derivative (**8d**) exhibited less potent activity than **8c**. This result indicates that the azole ring is desirable as a substituent for the ethylidene group for showing potent activity. On the other hand, the imidazo[4,5-*c*]pyridine (**8e**) and imidazo[4,5-*b*]pyridin-2-yl (**9**) derivatives were inactive. The large substituent extending between the 4 and 5 positions of the imidazole ring seems to be detrimental to antiresorptive activity.

The structure–activity relationships of this series, as described above, demonstrated that increase of lipophilicity is one means for increasing the antiresorptive activity, and that the position of the hydrophobic substituent is an important factor for determining the potency.

Compounds **4**, **5b** and **8b**, which showed a potent subcutaneous inhibitory effect in the PIH model, were evaluated for their oral inhibitory effects in the PIH model. Only **5b** exhibited an inhibitory effect at a dose of 1 mg/kg (**4**, **8b**: the minimum effective dose (MED)=3 mg/kg, data not shown). This result suggested that **5b** has better oral bioavailability than **4**. Compound **5b** was therefore selected for further pharmacological evaluation using the immobilization bone atrophy model in rats (DA model), as described in the Experimental

Table 5. Effects of Various Bisphosphonates in PIH and DA Models

Compd.	PIH model (MED,[a] mg/kg) s.c.	PIH model (MED,[a] mg/kg) *p.o.*	DA model (MED,[a] mg/kg) *p.o.*
Minodronate (**5b**)	0.003	≦1	1
Pamidronate (**1**)	0.3	300	100
Alendronate (**2**)	0.03	30	30
4	0.003	3	≦3

a) mg/kg, s.c.

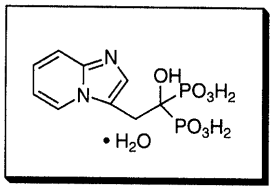

Fig. 6. Structure of Minodronate (YM529)

section. The results are described in Table 5. Compound **5b** was 30-fold and 100-fold more potent than alendronate (**2**) and pamidronate (**1**), respectively.

In conclusion, two new series of fused aza-heteroarylbisphosphonates and related compounds (**5, 6, 8, 9**) were synthesized and evaluated for their inhibitory activities on bone resorption using the PIH and DA models, for the purpose of finding a more potent bone resorption inhibitor. Among these compounds, [1-hydroxy-2-(imidazo[1,2-*a*]pyridin-3-yl)ethylidene]bisphosphonic acid (**5b**) showed the most potent inhibitory activity in not only the PIH model, but also the DA model. Based on these pharmacological evaluations, compound **5b** may be expected to be a useful drug for the treatment of disorders of bone mineral metabolism characterized by increased bone resorption, including Paget's disease, tumoral hypercalcemia, bone metastases and osteoporosis, and was selected for clinical development in the form of the monohydrate. Compound **5b** monohydrate is currently in clinical development under the designation YM529 (minodronate, Fig.6).

Experimental

All melting points were determined using a Yanaco micromelting point apparatus and are uncorrected. ^{1}H-Nuclear magnetic resonance (^{1}H-NMR) spectra were obtained with a JEOL JNM-EX90, JNM-FX100, JNM-FX270, JNM-EX400 or JNM-A500 spectrometer using $CDCl_3$, DMSO-d_6 or D_2O as the solvent. Chemical shifts are given in δ values (ppm) using tetramethylsilane (for $CDCl_3$ and DMSO-d_6) and sodium 3-(trimethylsilyl)propanoate-d_4 (for D_2O) as the internal standards, and coupling constants are given in Hz. Mass spectra (MS) were obtained with a JEOL JMS-DX300 or Hitachi M-80 mass spectrometer. Elemental analyses were carried out on a Yanaco MT-3 or MT-5 CHN analyzer and a Yokogawa IC7000S Ion Chromatoanalyzer. Column chromatography was performed using silica gel (Wakogel C-200) or ion exchange resin (Mitsubishi Chemical, DIAION®, HP20). Yields are not optimized. Spectral data for compounds **5**, **8** and **14** are shown in Tables 6, 7 and 8, respectively. Physical data for compounds **5** and **8** are shown in Tables 1 and 2, respectively.

General Procedure for the Synthesis of 1-Hydroxybisphosphonate Derivatives (5a—d). [1-Hydroxy-2-(imidazo[1,2-*a*]pyridin-2-yl)ethylidene]-bisphosphonic Acid (5a) A mixture of imidazo[1,2-*a*]pyridin-2-acetic acid (**10a**, 2.00 g, 11.3 mmol) and phosphorous acid (2.30 g, 28.0 mmol) in chlorobenzene (30 ml) was stirred at 110 °C for 30 min, and then phosphorus trichloride (3.5 ml, 40.1 mmol) was added dropwise. The whole was stirred at 115 °C for 6 h, and the solvent was removed by decantation. The residue was dissolved in 6 N HCl (30 ml), and the resulting mixture was stirred under reflux for 2 h. After removal of the solvent *in vacuo*, the residual oil was treated with a mixture of MeOH (30 ml) and acetone (30 ml). The precipitate was collected and recrystallized from 1 N HCl to give **5a** (1.98 g, 54.1%) as colorless pillars. The other compounds (**5b—d**) were prepared in a similar manner.

Benzyl (*E*)- 3-(Imidazo[1,2-*a*]pyridin-3-yl)acrylate (12) Benzyl dimethylphosphonoacetate (9.00 g, 34.9 mmol) was added dropwise to a suspension of NaH (60% dispersion in mineral oil, 1.40 g, 35.0 mmol) in *N,N*-dimethylformamide (DMF, 40 ml) and the resulting mixture was stirred at room temperature for 1.5 h. Imidazo[1,2-*a*]pyridin-3-carbaldehyde (**11**, 4.38 g, 30.0 mmol) was added, and the resulting mixture was stirred at room temperature for 1.5 h and then poured into ice-cold water. The colorless precipitate was filtered to give **12** (7.63 g, 91.5%). ^{1}H-NMR (DMSO-d_6): 5.25 (2H, s), 6.67 (1H, d, J=15.9 Hz), 6.98—7.85 (8 H, m), 8.07 (1H, d, J=15.9 Hz), 8.33 (1H, s), 8.89 (1H, d, J=6.8 Hz). FAB-MS *m/z*: 279 (MH^+).

3-(Imidazo[1,2-*a*]pyridin-3-yl)propanoic Acid (10d) A suspension of **12** (7.00 g, 25.2 mmol) and 10% palladium on carbon (0.53 g) in EtOAc (100 ml) and MeOH (50 ml) was hydrogenated under ordinary pressure at room temperature for 5 h. The reaction mixture was filtered to remove the catalyst, and the filtrate was evaporated *in vacuo*. The residue was chromatographed on silica gel using $CHCl_3$–MeOH–AcOH (20 : 2 : 1) as an eluent to give **10d** (1.90 g, 39.7%) as a pale yellow oil. ^{1}H-NMR (DMSO-d_6): 2.71 (2H, t, J=6.2 Hz), 3.11 (2H, t, J=6.2 Hz), 6.92 (1H, td, J=1.2, 6.8 Hz), 7.10—7.67 (3H, m), 8.36 (1H, d, J=6.8 Hz). EI-MS *m/z*: 190 (M^+).

[1-Hydroxy-2-(5,6,7,8-tetrahydroimidazo[1,2-*a*]pyridin-3-yl)ethylidene] bisphosphonic Acid (6) A suspension of **5b** (1.50 g, 4.41 mmol) and platinum oxide (0.30 g) in 0.7% aqueous HCl (50 ml) was hydrogenated at 50 psi for 1.5 h. The reaction mixture was filtered to remove the catalyst, and the filtrate was evaporated *in vacuo*. The residual oil was treated with a mixture of EtOH (30 ml) and acetone (50 ml). The precipitate was collected and recrystallized from H_2O–EtOH to give **6** (0.87 g, 61.0%) as colorless needles. mp 243—245 °C. ^{1}H-NMR (D_2O): 1.76—2.16 (4H, m), 2.90 (2H, t, J=6.0 Hz), 3.24 (2H, t, J=12.0 Hz), 3.96—4.24 (2H, t, J=6.0 Hz), 7.12 (1H, s). FAB-MS *m/z*: 327 (MH^+). *Anal.* Calcd for $C_9H_{16}N_2O_7P_2$: C, 33.14; H, 4.94; N, 8.59; P, 18.99. Found: C, 33.05; H, 4.92; N, 8.54; P, 18.86.

General Procedure for the Synthesis of Tetraalkylbisphosphonate Derivatives (14a—e). Tetraisopropyl [2-(2,3-dihydro-1*H*-imidazo[1,2-*a*]imidazol-1-yl)ethylidene]bisphosphonate (14d) A mixture of 2,3-dihydro-1*H*-imidazo[1,2-*a*]imidazole (**13d**, 0.60 g, 5.50 mmol) and tetraisopropyl ethenylidenebisphosphonate (2.00 g, 5.62 mmol) in tetrahydrofuran (THF, 2 ml) was stirred under reflux for 4 h, and the solvent evaporated *in vacuo*. The residue was chromatographed on silica gel using $CHCl_3$–MeOH (39 : 1) as the eluent to give **14d** (2.26 g, 88.3%) as a pale yellow oil. The other compounds (**14b**, **14c**, **14e**) were similarly prepared. Compound **14a** was also similarly prepared using tetraethyl ethenylidenebisphosphonate instead of tetraisopropyl ethenylidenebisphosphonate.

General Procedure for the Synthesis of Heteroarylalkylidenebisphosphonate Derivatives (8a—e). Method A. [2-(2,3-Dihydro-1*H*-imidazo[1,2-*a*]imidazol-1-yl)ethylidene]bisphosphonic Acid (8d) A solution of **14d** (0.90 g, 1.93 mmol) in concentrated HCl (15 ml) was stirred under reflux for 2 h, and the solvent evaporated *in vacuo*. The residual oil was treated with a mixture of MeOH (20 ml) and acetone (20 ml), and the precipitate was collected and recrystallized from H_2O–EtOH to give **8d** (0.49 g, 86.0%) as pale yellow needles. The other compounds (**8a—c**) were similarly prepared.

Method B. [2-(Imidazo[4,5-*c*]pyridin-3-yl)ethylidene]bisphosphonic Acid (8e) To an ice-cooled solution of **14e** (1.00 g, 2.10 mmol) in CCl_4 (20 ml) was added iodotrimethylsilane (1.25 ml, 8.75 mmol) dropwise, and the resulting mixture was stirred below 5 °C for 2.5 h. The reaction mixture was quenched by adding MeOH (30 ml), and then concentrated under reduced pressure. The residual oil was treated with a mixture of H_2O (1 ml) and MeOH (3 ml), and the precipitate was collected and recrystallized from H_2O–MeOH to give **8e** (0.22 g, 30.6%) as pale yellow needles.

Benzyl 3,3-Bis(diisopropoxyphosphoryl)propanoate (16) Tetraisopropyl methylenebisphosphonate (**15**, 10.00 g, 29.0 mmol) was added dropwise to a suspension of NaH (60% dispersion in mineral oil, 1.27 g, 31.7 mmol) in toluene (100 ml) with ice-bath cooling and the resulting mixture was stirred at room temperature for 2 h. Benzyl 2-bromoacetate (7.31 g, 31.9 mmol) was added, and the reaction mixture was stirred at room temperature overnight. After removal of the solvent *in vacuo*, the residue was partitioned between $CHCl_3$ and water. The organic phase was washed with brine, dried over $MgSO_4$, and evaporated to dryness *in vacuo*. The residue was chromatographed on silica gel using $CHCl_3$–MeOH (19 : 1) as an eluent to give **16** (8.66 g, 60.5%) as a colorless oil. ^{1}H-NMR($CDCl_3$): 1.32 (24H, d,

Table 6. Spectral Data for Bisphosphonates (**5**)

Compd.	^{1}H-NMR (D_2O), δ (ppm)	FAB-MS *m/z*
5a	3.53 (2H, t, *J*=12.6 Hz), 7.37 (1H, t, *J*=6.8 Hz), 7.79—7.88 (2H, m), 7.94 (1H, s), 8.57 (1H, d, *J*=6.8 Hz)	323 (MH^+)
5b	3.64 (2H, t, *J*=11.6 Hz), 6.88—7.70 (4H, m), 8.56 (1H, d, *J*=7.2 Hz)	323 (MH^+)
5c	2.46 (3H, s), 3.58 (2H, t, *J*=12.0 Hz), 6.92 (1H, t, *J*=7.6 Hz), 7.32 (1H, t, *J*=7.6 Hz), 7.44 (1H, t, *J*=7.6 Hz), 8.62 (1H, d, *J*=7.6 Hz)	337 (MH^+)
5d	2.30—2.43 (2H, m), 3.19—3.25 (2H, m), 7.04 (1H, td, *J*=1.0, 6.8 Hz), 7.38 (1H, ddd, *J*=1.0, 6.8, 9.8 Hz), 7.47 (1H, s), 7.57 (1H, dd, *J*=1.0, 9.8 Hz), 8.42 (1H, d, *J*=6.8 Hz)	337 (MH^+)

Table 7. Spectral Data for Bisphosphonates (**8**)

Compd.	^{1}H-NMR (D_2O), δ (ppm)	FAB-MS *m/z*
8a	2.39 (1H, tt, *J*=8.0, 20.0 Hz), 2.70 (3H, s), 4.26—4.72 (2H, m), 7.24 (1H, d, *J*=3.8 Hz), 7.46 (1H, d, *J*=3.8 Hz)	271(MH^+)
8b	2.31 (3H, s), 2.68 (1H, tt, *J*=7.0, 21.4 Hz), 4.59 (2H, td, *J*=6.9, 13.7 Hz), 7.28 (1H, s), 8.63 (1H, s)	271(MH^+)
8c	2.28 (1H, tt, *J*=7.2, 20.8 Hz), 3.24 (2H, td, *J*=7.2, 16.0 Hz), 6.88 (2H, s), 7.04 (2H, s)	296(MH^+)
8d	2.28 (1H, tt, *J*=7.2, 20.8 Hz), 3.50—3.96 (2H, m), 4.14 (4H, s), 6.74 (1H, d, *J*=2.2 Hz), 6.82 (1H, d, *J*=2.2 Hz)	298(MH^+)
8e	2.56 (1H, tt, *J*=7.2, 20.0 Hz), 4.56—5.04 (2H, m), 7.90 (1H, d, *J*=6.5 Hz), 8.40 (1H, d, *J*=6.5 Hz), 8.52 (1H, s), 8.90 (1H, s)	308(MH^+)

Table 8. Spectral Data for Bisphosphonates (**14**)

Compd.	R	Yield (%)	^{1}H-NMR($CDCl_3$), δ(ppm)	FAB-MS *m/z*
14a	Et	52.4	1.36(12H, t, *J*=7.2 Hz), 2.44 (3H, s), 2.72 (1H, tt, *J*=7.2, 23.4 Hz), 3.96—4.64 (10H, m), 6.88 (1H, d, *J*=2.8 Hz), 6.94 (1H, d, *J*=2.8 Hz)	383 (MH^+)
14b	iso-Pr	72.5	1.26—1.37 (24H, m), 2.19 (3H, s), 2.53 (1H, tt, *J*=5.5, 23.7 Hz), 4.40 (2H, td, *J*=5.4, 15.0 Hz), 6.71 (1H, s), 7.42 (1H, s)	439 (MH^+)
14c	iso-Pr	46.5	1.10—1.50 (24H, m), 2.56 (1H, tt, *J*=7.2, 24.0 Hz), 3.34 (2H, td, *J*=7.2, 16.0 Hz), 4.52—5.04 (4H, m), 6.80 (1H, s), 6.96—7.16 (3H, m)	464 (MH^+)
14d	iso-Pr	88.3	1.36 (24H, d, *J*=7.0 Hz), 2.96 (1H, tt, *J*=7.2, 23.2 Hz), 3.56—4.00 (2H, m), 3.94 (4H, s), 4.56—5.06 (4H, m), 6.53 (1H, d, *J*=2.4 Hz), 6.68 (1H, d, *J*=2.4 Hz)	466 (MH^+)
14e	iso-Pr	43.5	1.12—1.48 (24H, m), 2.72 (1H, tt, *J*=7.2, 23.0 Hz), 4.52—5.04 (6H, m),7.48 (1H, d, *J*=6.5 Hz), 8.08 (1H, s), 8.48 (1H, d, *J*=6.5 Hz), 9.12 (1H, s)	476 (MH^+)

J=6.2 Hz), 2.60—3.11 (3H, m), 4.56—5.00 (4H, m), 5.15 (2H, s), 7.36 (5H, s). FAB-MS *m/z*: 493 (MH^+).

3,3-Bis(diisopropoxyphosphoryl)propanoic Acid (17) A suspension of **16** (3.00 g, 6.09 mmol) and 10% palladium on carbon (0.47 g) in EtOAc (30 ml) was hydrogenated under ordinary pressure at room temperature for 20 min. The reaction mixture was filtered to remove the catalyst, and the filtrate was evaporated *in vacuo*. The residue was chromatographed on silica gel using $CHCl_3$–MeOH (9 : 1) as the eluent to give **17** (2.28 g, 93.0%) as a colorless oil. ^{1}H-NMR($CDCl_3$): 1.34 (24H, d, *J*=6.2 Hz), 2.55—3.12 (3H, m), 4.55—5.02 (4H, m), 8.09 (1H, brs). FAB-MS (neg.) *m/z*: 401 $(M-H)^-$.

[2-(1*H*-Imidazo[4,5-*b*]pyridin-2-yl)ethylidene]bisphosphonic Acid (9) A mixture of **17** (1.90 g, 4.72 mmol), 2,3-diaminopyridine (0.55 g, 5.04 mmol) and 75% polyphosphoric acid (PPA, 10 ml) was stirred at 100 °C for 3 h. The reaction mixture was poured onto crushed ice, and then concentrated under reduced pressure. The residue was chromatographed on an ion exchange resin using H_2O–MeOH (19:1) as the eluent. The desired fractions were collected and evaporated *in vacuo*. The residual oil was treated with acetone (10 ml), and the precipitate was collected and recrystallized from H_2O to give **9** (0.30 g, 18.1%) as colorless needles. mp 238—240 °C. ^{1}H-NMR(D_2O): 2.04—3.16 (3H, m), 6.80 (1H, dd, *J*=5.5, 7.2 Hz), 7.54 (1H, dd, *J*=2.0, 7.2 Hz), 7.92 (1H, dd, *J*=2.0, 5.5 Hz). FAB-MS *m/z*: 308 (MH^+). *Anal.* Calcd for $C_8H_{11}N_3O_6P_2 \cdot 2.5\ H_2O$: C, 27.28; H, 4.58; N, 11.93; P, 17.59. Found: C, 27.42; H, 4.40; N, 12.16; P, 17.59.

X-Ray Crystallographic Analysis of 5a Single crystals of **5a**, grown from H_2O–EtOH, were used for data collection on a Rigaku AFC-7R diffractometer using CuK_α at room temperature. The crystal data were determined as follows: $C_9H_{12}N_2O_7P_2$, M.W.=322.15, monoclinic, space group $P2_1/c$, a=9.119 (1) Å, b=10.331(1) Å, c=13.387 (1) Å, β=103.61 (1)°, Z=4, D_c=1.746 g/cm^3. A total of 2771 reflections, of which 2603 were unique, were measured in the 2θ angle range up to 153.4°. The structure was solved by direct methods using program SIR92.[23] The refinements were first carried out isotropically, then anisotropically for the non-hydrogen atoms, with the positions of the hydrogen atoms fixed. The *R*-factor and weighted *R*-factor were 0.039 and 0.063, respectively, for 2113 reflections with $I>3\sigma(I)$. All calculations were performed using program TEXSAN.[24]

X-Ray Crystallographic Analysis of 5b Monohydrate Single crystals of **5b** monohydrate, grown from 1 N HCl, were used for the data collection on a Rigaku AFC-5R diffractometer using CuK_α at room temperature. Crystal data was determined as follows: $C_9H_{12}N_2O_7P_2 \cdot H_2O$, M.W.=340.17, triclinic, space group $P\bar{1}$, a=8.971 (1) Å, b=9.963(1) Å, c=7.362 (9) Å, α=102. 77(1)°, β=91.40 (1)°, γ=75.00 (1)°, Z=2, D_c=1.823g/cm^3. A total of 2597 reflections, of which 2435 were unique, were measured in the 2θ angle range up to 150.0°. The structure was solved by direct methods using the program SHELX86.[25] The refinements were first carried out isotropically, then anisotropically for non-hydrogen atoms, with the positions of the hydrogen atoms fixed. The *R*-factor and weighted *R*-factor are 0.051 and 0.099, respectively, for 2205 reflections with $I>2\sigma(I)$. All calculations were performed using the program TEXSAN.[24]

Molecular Modeling Study The structure of compound **5c** was generated by adding a methyl group to the crystal structure of compound **5b** monohydrate. The orientations of the methyl hydrogen atoms were adjusted by rotating the torsion angle in such a way that the hydrogen atoms did not interact with the neighboring OH group. The conformational energy of **5c** was examined by a systematic search using two rotatable bonds, C8–C9–

C10–C11 and C9–C10–C11–O12. The two torsion angles were changed from 0° to 360° in increments of 3° and the conformational energy was then calculated for every conformer. Electrostatic interactions were not included in the energy calculations. The same calculations were also carried out for the crystal structure of **5b** monohydrate. All calculations were performed using the SYBYL molecular modeling software.[21]

Authentic Materials Compounds **1**, **2**, **4** and **7** were prepared in our company according to the methods described in the literature.[8—10,26]

Pharmacological Methods. Antiresorptive Activity Reduction in Serum Ca^{2+} Concentration in Rats (PIH Model): The test compound was administered subcutaneously or orally to rats (Wistar, male, 5-week-old, $n=5$). After 3 d, PTH (synthetic human 1—34, 30 μg/kg) was given intravenously. A blood sample was then collected with a vacuum tube 45 min after PTH injection. The free Ca (Ca^{2+}) concentration in serum was measured with an electrolyte analyzer (sera 252, Horiba Manufacturing Co., Ltd.). The results are expressed as MED (mg/kg). Statistical significance of the value was analyzed using a one-way ANOVA test ($p<0.05$).

Inhibition of Decrease in Dry Weight of the Bone in Rats (DA model): In rats (Wistar, male, 5-week-old, $n=5$), a 4 mm or longer section of the left brachial plexus was excited to immobilize the left forelimb. The test compound was administered orally every day for two weeks after immobilization and then the left humerus was removed. After the bone was dehydrated and defatted with alcohol and acetone, its dry weight was measured. The results are expressed as the MED (mg/kg). Statistical significance of this value was analyzed using a one-way ANOVA test ($p<0.05$).

Acknowledgments We are grateful to Drs. Kiyoshi Murase, Tetsushi Abe and Hiroyuki Motoie for their valuable suggestions and to the staff of the pharmacology laboratories for biological evaluation. Our thanks are also due to the staff of the molecular chemistry research laboratory for measurement of ^{1}H-NMR and MS spectra and the elemental analyses.

References and Notes

1) Part I: Takeuchi M., Sakamoto S., Yoshida M., Abe T., Isomura Y., *Chem. Pharm. Bull.*, **41**, 688—693 (1993).
2) Part of this work was presented at *the 203th National Meeting, American Chemical Society*, San Francisco, April 1992, Medicinal Chemistry 208.
3) Hughes D. E., Mian M., Guilland-Cumming D.F., Russell R. G. G., *Drug Exp. Clin. Res.*, **17**, 109—114 (1991).
4) Fleisch H., *Bone*, **8** (Suppl. 1), 523—528 (1987).
5) Susan M. O., *J. Bone Min. Res.*, **8**, 597—606 (1988), and references cited therein.
6) Motoie H., Nakamura T., O'uchi N., Nishikawa H., Kanoh H., Abe T., Kawashima H., *J. Bone Min. Res*, **10**, 910—920 (1995).
7) Hiraga T., Tanaka S., Yamamoto M., Nakajima T., Ozawa H., *Bone*, **18**, 1—7 (1996).
8) Bosies M., Gall R., DE 3626058, (1988) [*Chem. Abstr.*, **108**, 186996*f* (1988)].
9) Jaeggi K. A., Widler L., Japan. Patent, 63150291 (1988) [*Chem. Abstr.*, **110**, 24084*w* (1989)].
10) Krueger F., Bauer L., Michel W., DE 2130794 (1973) [*Chem. Abstr.*, **78**, 84528*z* (1973)].
11) Casagrande A., Invernizzi G., Ferrari G., *Farmaco Ed. Sci.*, **23**, 1141—1148 (1968).
12) Abignente E., Arena F., Luraschi E., Saturnino C., Marno E., Russo S., Magliulo R., *Farmaco Ed. Sci.*, **41**, 119—130 (1986).
13) Almirante L., Mugnaini A., Rugarli P., Gamba A., Zefelippo E., Toma N. D., Murmann W., *J. Med. Chem.*, **12**, 122—126 (1969).
14) Almirante L., Mugnaini A., Toma N. D., Gamba A., Murmann W., Hidalgo J., *J. Med. Chem.*, **13**, 1048—1051 (1970).
15) Compernolle F., Toppet S., *J. Heterocycl. Chem.*, **23**, 541—544 (1986).
16) Arya V. P., Nagarajan K., David J., Shenoy S. J., Gokhale N. G., *Indian J. Chem., Sect. B*, **16**, 226—230 (1978).
17) Allen S. K., Raymond F. B., *J. Heterocycl. Chem.*, **27**, 563—566 (1990).
18) Degenhardt C. R., Burdsall D. C., *J. Org. Chem.*, **51**, 3488—3490 (1986).
19) The clogP values were calculated using clogP for Windows Ver. 1.0.0, BioByte Corporation, 201 West 4th St., Suite 204, Claremont, CA 91711.
20) Insight II Ver. 97.0, Molecular Simulations Inc., 9685 Scranton Road, San Diego, CA 92121, U.S.A..
21) SYBYL molecular modeling software, Tripos Inc., St. Louis, MO, U.S.A..
22) The angles of the least squares planes were calculated using the program LISTUP, Takenaka A., *J. Cryst. Soc. Jpn.*, **32**, 323—325 (1990).
23) Altomare A., Cascarano M., Giacovazzo C., Guagliardi A., Burla M. C., Polidori G., Camalli M., *J. Appl. Cryst.*, **27**, 435—436 (1994).
24) Molecular Structure Corporation, TEXAN. TEXTRAY structure analysis package, MSC 3200 Research Forest Drive, The Woodland, TX 77831 U.S.A. (1985).
25) Sheldrick G. M., SHELX86. Program for the solution of crystal structures, University of Göttingen, Germany (1985).
26) Blum H., Worms K. H., DE 3016289 (1981) [*Chem. Abstr.*, **96**, 52503*t* (1982)].